J. Plasma Phys. (2023), *vol.* 89, 905890109
Published by Cambridge University Press
doi:10.1017/S0022377823000016

Effect of temperature anisotropy on the dynamics of geodesic acoustic modes

J.N. Sama [1,†], A. Biancalani [2,3], A. Bottino [3], I. Chavdarovski [4], D. Del Sarto [1], A. Ghizzo [1], T. Hayward-Schneider [3], Ph. Lauber [3], B. Rettino [3] and F. Vannini [3]

[1]Institut Jean Lamour UMR 7198, Université de Lorraine-CNRS, Nancy 54011, France

[2]Léonard de Vinci Pôle Universitaire, Research Center, Paris La Défense 92400, France

[3]Max Planck Institute for Plasma Physics, Garching 85748, Germany

[4]Korea Institute of Fusion Energy, Daejeon 34133, South Korea

(Received 11 October 2022; revised 26 December 2022; accepted 30 December 2022)

In this work, we revisit the linear gyro-kinetic theory of geodesic acoustic modes (GAMs) and derive a general dispersion relation for an arbitrary equilibrium distribution function of ions. A bi-Maxwellian distribution of ions is then used to study the effects of ion temperature anisotropy on GAM frequency and growth rate. We find that ion temperature anisotropy yields sensible modifications to both the GAM frequency and growth rate as both tend to increase with anisotropy and these results are strongly affected by the electron to ion temperature ratio.

Key words: fusion plasma, plasma instabilities, plasma simulation

1. Introduction

Geodesic acoustic modes (GAMs) (Winsor, Johnson & Dawson 1968) are oscillating axisymmetric perturbations that are unique to configurations with closed magnetic field lines with a geodesic curvature, like tokamaks. They are the oscillating counterparts of the zero-frequency zonal flow (Hasegawa, Maclennan & Kodama 1979) and are examples of zonal structures. Zonal structures are of great interest to magnetic fusion reactors due to their potential capabilities of generating nonlinear equilibrium (Chen & Zonca 2007) by regulating microscopic turbulence and its associated heat and particle transport.

Geodesic acoustic modes have been largely studied in the literature, both analytically (see Garbet *et al.* 2006; Smolyakov *et al.* 2008; Zonca & Chen 2008; Qiu, Chen & Zonca 2009; Chakrabarti *et al.* 2010; Zhang & Zhou 2010; Hassam & Kleva 2011; Zarzoso *et al.* 2012; Gao 2013; Girardo *et al.* 2014; Ren 2015; Ming, Zhou & Wamg 2018; Conway, Smolyakov & Ido 2022) and numerically (see Biancalani *et al.* 2014; Novikau *et al.* 2017; Grandgirard *et al.* 2019). A key aspect in the linear gyro-kinetic theory of GAMs is the determination of mode frequency and damping rate. The GAM frequency is of the order of the ion sound frequency, and its major damping mechanism is collisionless damping. Analytical expressions of GAM frequency and growth rate can be found, for example,

† Email address for correspondence: juvert-njeck.sama@univ-lorraine.fr

in Sugama & Watanabe (2006) and Qiu *et al.* (2009). These expressions were obtained assuming Maxwellian distributions of ions and electrons with no temperature anisotropy.

Tokamak plasmas are generally modelled in analytical theory, assuming isotropic Maxwellian distributions of ions and electrons. However, in reality, there can be several sources of anisotropy in tokamak plasmas. Anisotropy in tokamaks can be introduced by auxiliary heating such as neutral beam injection, which can generate a strong parallel temperature anisotropy, whereas strong perpendicular temperature anisotropy can be observed when using ion cyclotron resonance heating. Parallel and perpendicular here are defined with respect to the equilibrium magnetic field. Generally, ion temperature anisotropy, both gyro-tropic and non-gyro-tropic, can be generated due to the action of the traceless rate of shear, which anisotropically heats the in-plane components of the pressure tensor by tapping kinetic energy from shear flow when the local gradient of the ion fluid velocity, say $\omega \sim \|\nabla \boldsymbol{u}_i\|$, is not negligible with respect to the local ion cyclotron frequency $\varOmega_i$ and the collision rate (Del Sarto, Pegoraro & Califano 2016). This condition is likely to occur in developed turbulence, since it can be verified on vorticity sheets delimiting vortex structures (Del Sarto & Pegoraro 2018*a*). In particular, as long as the ratio $\omega/\varOmega_i$ remains small enough, the generated anisotropy is mostly gyro-tropic and thus compatible with a gyro-kinetic description (Del Sarto & Pegoraro 2018*b*) and it can be thus related to the first-order finite-Larmor radius corrections to double-adiabatic closures (Kaufman 1960; Thompson 1961; Macmahon 1965; Cerri *et al.* 2013). Sasaki *et al.* (1997) measured reasonably high ion temperature anisotropy in EXTRAP-T2, and large pressure anisotropies have also been reported in Hole *et al.* (2001) and Hole *et al.* (2011). Ren & Cao (2014) studied the impact of ion temperature anisotropy on GAM frequency and growth rate in the limit of a vanishing electron to ion temperature ratio, with ions described by a bi-Maxwellian distribution. Those authors found that ion temperature anisotropy modifies the linear dynamics of GAMs. However, the GAM dynamics is known to strongly depend on the electron to ion temperature ratio (see Sugama & Watanabe 2006; Zonca & Chen 2008; Qiu *et al.* 2009; Biancalani *et al.* 2014). Hence, a finite electron to ion temperature ratio must be retained in a complete linear theory of GAMs.

In this work, we investigate the linear dynamics of GAMs with a bi-Maxwellian distribution of ions and assuming adiabatic electrons, as in Zonca & Chen (2008) and Sugama & Watanabe (2006). We generalize the work of Ren & Cao (2014) to a general value of electron to ion temperature ratio and by keeping account of a gyro-tropic ion temperature anisotropy, using an approach based on the standard limit of small finite orbit radius and small finite orbit width, kept up to the leading order (consistently with Zonca, Chen & Santoro (1996) and Zonca & Chen (2008)). We show that in the appropriate limits, we recover the GAM dispersion derived in Ren & Cao (2014), Zonca & Chen (2008) and Girardo *et al.* (2014) from the general GAM dispersion relation which we here obtain. From our study, we find that the ion temperature anisotropy yields a sensible modification to both the real and imaginary parts of the frequency, as both tend to be increasing functions of $\chi = T_{\perp,i}/T_{\parallel,i}$, and this result is strongly affected by the electron to ion temperature ratio, $\tau = T_e/T_i$. The equivalent ion temperature T_i is defined such that it corresponds to the same total pressure as that of the anisotropic distribution ($T_i = T_{\parallel,i}/3 + 2T_{\perp,i}/3$).

This first section is an introduction, which describes the motivations for this work. In § 2, we derive a general linear GAM dispersion relation for an arbitrary distribution function. In § 3, we solve the dispersion relation with a bi-Maxwellian distribution of ions and study the impact of ion temperature anisotropy and electron to ion temperature ratio on GAM frequency and growth rate. We apply our theory to an experimentally relevant case in § 4 and conclusions are reported in § 5.

2. The model for a general distribution function

In this section, we use the gyro-kinetic formalism to study the physics of GAMs in the electrostatic limit. The fundamental equations of this model are the gyro-kinetic Vlasov equation (2.1) and Poisson equations (2.2):

$$\frac{\partial f_s}{\partial t} + \dot{\boldsymbol{R}} \cdot \frac{\partial f_s}{\partial \boldsymbol{R}} + \dot{E}\frac{\partial f_s}{\partial E} = 0, \tag{2.1}$$

$$-\nabla \cdot \left(\frac{n_{0,i} m_i c^2}{B^2} \nabla_\perp \Phi \right) = \int \mathrm{d}W_i Z_i e J_{0,i} f_i - \int \mathrm{d}W_e e f_e, \tag{2.2}$$

where f_s is the distribution function of a given species, $\boldsymbol{R}$ the particle position vector, $E = (m_s/2)(v_\parallel^2 + v_\perp^2)$ the particle energy, e the electron charge, $n_{0,s}$ the equilibrium density of a species s, m the particle mass, c the speed of light, B the magnitude of magnetic field, Z_s the species charge number, $J_{0,i}$ the ion gyro-average operator and $\mathrm{d}W_s$ a volume element in velocity space.

We make the following assumptions:

(i) We consider adiabatic electrons.
(ii) We neglect magnetic fluctuations.
(iii) We use flat density and temperature profiles.

2.1. *Linear analysis*

We linearize the Vlasov and quasi-neutrality equations by splitting each quantity into an equilibrium and a perturbed component, such that

$$f_s = f_{0,s} + f_{1,s}, \tag{2.3}$$

$$\dot{\boldsymbol{R}} = \dot{\boldsymbol{R}}_0 + \dot{\boldsymbol{R}}_1, \tag{2.4}$$

$$\dot{E} = \dot{E}_0 + \dot{E}_1, \tag{2.5}$$

$$\Phi = \Phi_1, \tag{2.6}$$

where $\dot{\boldsymbol{R}}_0$ is the unperturbed particle velocity, i.e. $\dot{\boldsymbol{R}}_0 = \boldsymbol{v}_\parallel + \boldsymbol{v}_{\nabla B} + \boldsymbol{v}_{curvB}$, and $E_0 = (m(v_\parallel^2 + v_\perp^2))/2$.

2.2. *Linear Vlasov equation*

Substituting (2.3)–(2.6) in (2.1), and neglecting second- and higher-order terms, the linear Vlasov equation reads

$$\frac{\partial f_{1,s}}{\partial t} + \dot{\boldsymbol{R}}_0 \cdot \frac{\partial f_{1,s}}{\partial \boldsymbol{R}} = -\dot{E}_1 \frac{\partial f_{0,s}}{\partial E}. \tag{2.7}$$

This linear Vlasov equation can be further simplified by splitting the perturbed distribution function into an adiabatic and a non-adiabatic component:

$$f_{1,s} = E_1 \frac{\partial f_{0,s}}{\partial E} + h_s. \tag{2.8}$$

Substituting (2.8) in (2.7), we obtain the equation for the non-adiabatic part of the perturbed distribution function:

$$\frac{\partial h_s}{\partial t} + \dot{\boldsymbol{R}}_0 \cdot \frac{\partial h_s}{\partial \boldsymbol{R}} = -\dot{E}_1 \frac{\partial f_{0,s}}{\partial E}. \tag{2.9}$$

Using the expression of the equilibrium velocity and perturbations of the form $x \longrightarrow \exp(\mathrm{i}k_r - \mathrm{i}\omega t) + \mathrm{c.c.}$ in (2.9), we obtain the expression

$$\left(\omega_{t,s}\frac{\partial}{\partial\theta} - \mathrm{i}(\omega + \omega_{d,s})\right) h_s = \mathrm{i}\omega E_1 \frac{\partial f_{0,s}}{\partial E}, \tag{2.10}$$

where $\omega_t = v_\parallel / qR_0$ is the transit frequency, q is the safety factor, $\omega_{d,s} = \bar{\omega}_{d,s}\sin\theta$ is the drift frequency, with $\bar{\omega}_{d,s} = (cm_s k_r / Z_s e B_0 R_0)(v_\parallel^2 + v_\perp^2/2)$, $E_1 = Z_s e J_{0,s}\Phi_1$ and k_r is the radial wavenumber. Since GAMs are predominantly zonal, we can further divide the non-adiabatic part of the perturbed distribution function into a zonal and a non-zonal part:

$$h = \bar{h} + \delta h. \tag{2.11}$$

Similarly, we write the scalar potential as

$$\Phi_1 = \bar{\Phi} + \tilde{\Phi}, \tag{2.12}$$

where the overbar represents the zonal components. Using these definitions, and making a flux surface average of the gyro-kinetic equation to eliminate the zonal component of the non-adiabatic part of the perturbed distribution function, the linear Vlasov equation reduces to

$$\left(\omega_{t,s}\frac{\partial}{\partial\theta} - \mathrm{i}(\omega + \omega_{d,s})\right) \delta h_s = \mathrm{i}Z_s \frac{\partial f_{0,s}}{\partial E}\left(\omega J_{0,s}\tilde{\Phi} - \omega_{d,s} J_{0,s}\bar{\Phi}\right). \tag{2.13}$$

The corresponding vorticity equation is obtained by multiplying this relation by the gyro-average operator and integrating over the velocity space:

$$\left\langle J_{0,s}\left(\omega_{t,s}\frac{\partial}{\partial\theta} - \mathrm{i}(\omega + \omega_{d,s})\right)\delta h_s\right\rangle_W = \left\langle \mathrm{i}Z_s\frac{\partial f_{0,s}}{\partial E}\left(\omega J_{0,s}^2\tilde{\Phi} - \omega_{d,s}J_{0,s}^2\bar{\Phi}\right)\right\rangle_W. \tag{2.14}$$

Considering all the changes of variable we have made, the perturbed distribution function has the form

$$f_{1,s} = Z_s e J_{0,s}\frac{\partial f_{0,s}}{\partial E}\tilde{\Phi} + \delta h_s. \tag{2.15}$$

2.3. *Linear quasi-neutrality equation*

Using a similar approach, we substitute (2.3) and (2.6) into (2.2) and we thus obtain the following equation:

$$\frac{m_i c^2}{B^2}k_r^2\bar{\Phi} = e^2\left\langle J_{0,i}^2\frac{\partial f_{0,i}}{\partial E}\right\rangle_W \left(1 + \frac{\left\langle J_{0,e}^2\dfrac{\partial f_{0,e}}{\partial E}\right\rangle_W}{\left\langle J_{0,i}^2\dfrac{\partial f_{0,i}}{\partial E}\right\rangle_W}\right)\tilde{\Phi} + e\left\langle J_{0,i}\delta h_i\right\rangle_W, \tag{2.16}$$

where $\langle\cdots\rangle_W$ represents the integral over velocity space. The non-adiabatic part of the perturbed electron distribution function has been neglected in accordance with our assumptions.

https://doi.org/10.1017/S0022377823000016 Published online by Cambridge University Press

2.4. *Ordering of the gyro-kinetic equation*

The gyro-kinetic equation (2.13) describes a wide range of phenomena at different time scales. In order to study GAMs, we need to apply an appropriate ordering that will filter out time scales which are irrelevant to GAM dynamics. The GAM frequency is of the order of ion sound frequency. The ordering is done by comparing this frequency with the characteristic frequencies in our system, i.e. $\omega_{t,s}$, $\omega_{d,s}$:

$$\frac{\omega_{t,i}}{\omega} \sim O(1), \quad \frac{\omega_{d,i}}{\omega} \sim O(\epsilon), \quad \frac{\delta h_i}{f_{0,i}} \sim O(\epsilon), \tag{2.17a–c}$$

$$\frac{\omega_{t,e}}{\omega} \gg 1, \quad \frac{\omega_{d,e}}{\omega} \sim O(1), \quad \frac{\delta h_e}{f_{0,e}} \sim O(\epsilon). \tag{2.18a–c}$$

To leading order, the ion and electron gyro-kinetic equations are, respectively,

$$\left(\frac{\omega_{t,i}}{\omega}\frac{\partial}{\partial\theta} - \mathrm{i}\right)\delta h_i = \mathrm{i}Z_i e\frac{\partial f_{0,i}}{\partial E}\left(J_{0,i}\tilde{\Phi} - J_{0,i}\frac{\omega_{d,i}}{\omega}\bar{\Phi}\right), \tag{2.19}$$

$$\delta h_e = 0. \tag{2.20}$$

2.5. *General form of dispersion relation*

We consider the following form for the non-zonal perturbed ion distribution function and scalar potential:

$$\tilde{\Phi} = \tilde{\Phi}_s \sin\theta + \tilde{\Phi}_c \cos\theta, \tag{2.21}$$

$$\delta h_i = \delta h_{i,s} \sin\theta + \delta h_{i,c} \cos\theta. \tag{2.22}$$

Substituting these relations into (2.19) and separating the sine and cosine components, we obtain

$$\delta h_{i,s} = \frac{\mathrm{i}Z_i J_{0,i}\dfrac{\partial f_{0,i}}{\partial E}}{\left(\dfrac{\omega_{t,i}}{\omega}\right)^2 - 1}\left[-\mathrm{i}\left(\tilde{\Phi}_s - \left(\frac{\bar{\omega}_{d,i}}{\omega}\right)\bar{\Phi}\right) + \frac{\omega_{t,i}}{\omega}\tilde{\Phi}_c\right], \tag{2.23}$$

$$\delta h_{i,c} = -\frac{\mathrm{i}Z_i J_{0,i}\dfrac{\partial f_{0,i}}{\partial E}}{\left(\dfrac{\omega_{t,i}}{\omega}\right)^2 - 1}\left[\frac{\omega_{t,i}}{\omega}\left(\tilde{\Phi}_s - \left(\frac{\bar{\omega}_{d,i}}{\omega}\right)\bar{\Phi}\right) + \mathrm{i}\tilde{\Phi}_c\right]. \tag{2.24}$$

https://doi.org/10.1017/S0022377823000016 Published online by Cambridge University Press

Following the same procedure with the quasi-neutrality equation:

$$\tilde{\Phi}_c = -\frac{\langle J_{0,i}\delta h_{i,c}\rangle_W}{e\left\langle J_{0,i}^2 \frac{\partial f_{0,i}}{\partial E}\right\rangle_W \left(1 + \frac{\left\langle J_{0,e}^2 \frac{\partial f_{0,e}}{\partial E}\right\rangle_W}{\left\langle J_{0,i}^2 \frac{\partial f_{0,i}}{\partial E}\right\rangle_W}\right)}, \tag{2.25}$$

$$\tilde{\Phi}_s = -\frac{\langle J_{0,i}\delta h_{i,s}\rangle_W}{e\left\langle J_{0,i}^2 \frac{\partial f_{0,i}}{\partial E}\right\rangle_W \left(1 + \frac{\left\langle J_{0,e}^2 \frac{\partial f_{0,e}}{\partial E}\right\rangle_W}{\left\langle J_{0,i}^2 \frac{\partial f_{0,i}}{\partial E}\right\rangle_W}\right)}. \tag{2.26}$$

Taking the flux surface average of the quasi-neutrality equation (2.19) and the vorticity equation (2.14), we have, respectively,

$$\frac{m_i c^2}{B^2} k_r^2 \bar{\Phi} = e\overline{\langle J_{0,i}\delta h_i\rangle}_W, \tag{2.27}$$

$$\overline{\langle J_{0,i}\delta h_i\rangle}_W = -\frac{\overline{\langle J_{0,i}\omega_{d,i}\delta h_i\rangle}_W}{\omega}. \tag{2.28}$$

Substituting (2.28) into (2.27) and evaluating the flux surface average, we obtain

$$\frac{2m_i}{B^2} k_r^2 \bar{\Phi} = -\frac{e}{c^2\omega}\left\langle J_{0,i}\bar{\omega}_{d,i}\delta h_{i,s}\right\rangle. \tag{2.29}$$

Substituting (2.23), we obtain the general dispersion relation of GAMs to leading order:

$$\frac{2m_i c^2 k_r^2}{B^2}\bar{\Phi} = -e^2\omega\left\langle \frac{J_{0,i}^2\bar{\omega}_{d,i}\frac{\partial f_{0,i}}{\partial E}}{\omega_{t,i}^2 - \omega^2}\right\rangle_W \tilde{\Phi}_s + e^2\left\langle \frac{J_{0,i}^2\bar{\omega}_{d,i}^2\frac{\partial f_{0,i}}{\partial E}}{\omega_{t,i}^2 - \omega^2}\right\rangle_W \bar{\Phi}. \tag{2.30}$$

3. Bi-Maxwellian case

3.1. *Derivation of dispersion relation*

To evaluate the integrals over the velocity space given in the general linear GAM dispersion relation equation (2.30), we have to choose an equilibrium distribution function for ions. In this work, we consider it to be a bi-Maxwellian, while a regular Maxwellian is used for electrons. The ion distribution function is normalized such that its integral over velocity space equals one ($n_{0,i} = 1$). We take $J_{0,i} = 1$ (drift kinetic limit):

$$f_{0,i} = \left(\frac{m_i}{2\pi T_\parallel}\right)^{1/2}\left(\frac{m_i}{2\pi T_\perp}\right)\exp\left[-\frac{m_i}{2}\left(\frac{v_\parallel^2}{T_\parallel} + \frac{v_\perp^2}{T_\perp}\right)\right]. \tag{3.1}$$

By defining an equivalent temperature, $T_i = T_{\parallel,i}/3 + 2T_{\perp,i}/3$, the bi-Maxwellian can be written in the form

$$f_{0,i} = \frac{b^{3/2}}{\pi^{3/2} v_t^3 \chi}\exp\left[-b\left(\frac{v_\parallel^2 + v_\perp^2\chi^{-1}}{v_t^2}\right)\right], \tag{3.2}$$

https://doi.org/10.1017/S0022377823000016 Published online by Cambridge University Press

where $b = (2\chi + 1)/3$, with $\chi = T_{\perp,i}/T_{\parallel,i}$, $v_t = \sqrt{2T_i/m}$ and $E = (m/2)(v_\parallel^2 + v_\perp^2)$. We have

$$\frac{\partial f_{0,i}}{\partial E} = -\frac{b}{T_i} f_{0,i}. \tag{3.3}$$

Equation (2.26) then reduces to

$$\tilde{\Phi}_s = \frac{\omega \left\langle \dfrac{\bar{\omega}_{d,i} f_{0,i}}{\omega_t^2 - \omega^2} \right\rangle_W}{1 + \dfrac{1}{\tau b} + \omega^2 \left\langle \dfrac{f_{0,i}}{\omega_t^2 - \omega^2} \right\rangle_W} \bar{\Phi}, \tag{3.4}$$

where $\tau = T_e/T_i$. Substituting this result in the general dispersion relation, we have

$$\frac{2m_i c^2 k_r^2}{B^2} + \frac{e^2 b}{T_i} \left[\left\langle \frac{\bar{\omega}_{d,i}^2 f_{0,i}}{\omega_t^2 - \omega^2} \right\rangle_W - \frac{\omega^2 \left\langle \dfrac{\bar{\omega}_{d,i} f_{0,i}}{\omega_t^2 - \omega^2} \right\rangle_W^2}{1 + \dfrac{1}{\tau b} + \omega^2 \left\langle \dfrac{f_{0,i}}{\omega_t^2 - \omega^2} \right\rangle_W} \right] = 0. \tag{3.5}$$

These three velocity integrals once evaluated read

$$\left\langle \frac{\bar{\omega}_{d,i} f_{0,i}}{\omega_t^2 - \omega^2} \right\rangle_W = \frac{c m_i k_r v_t^2}{e B_0 R_0 b \omega_0^2 y} \left[y + \left(\frac{\chi}{2} + y^2 \right) Z(y) \right], \tag{3.6}$$

$$\left\langle \frac{\bar{\omega}_{d,i}^2 f_{0,i}}{\omega_t^2 - \omega^2} \right\rangle_W = \left(\frac{c m_i k_r v_t^2}{e B_0 R_0 b} \right)^2 \frac{1}{\omega_0^2 y} \left[\frac{y}{2} + y^3 + y\chi + \left(\frac{\chi^2}{2} + \chi y^2 + y^4 \right) Z(y) \right], \tag{3.7}$$

$$\left\langle \frac{f_{0,i}}{\omega_t^2 - \omega^2} \right\rangle_W = \frac{1}{\omega_0^2} \frac{Z(y)}{y}, \tag{3.8}$$

where $Z(y)$ is the plasma dispersion function and

$$y = \frac{\omega}{\omega_0}, \quad \omega_0 = \frac{v_t}{q R_0 \sqrt{b}}. \tag{3.9a,b}$$

Then (3.5) becomes

$$y + q^2 \left[F(y) - \frac{N^2(y)}{D(y)} \right] = 0, \tag{3.10}$$

with

$$F(y) = \frac{y}{2} + y^3 + y\chi + \left(\frac{\chi^2}{2} + y^2 \chi + y^4 \right) Z(y), \tag{3.11}$$

$$N(y) = y + \left(\frac{\chi}{2} + y^2 \right) Z(y), \tag{3.12}$$

$$D(y) = \frac{1}{y} \left(1 + \frac{1}{\tau b} \right) + Z(y). \tag{3.13}$$

3.2. *Comparison with fluid limit and with previous results*

In the limit $\chi = 1$, we recover the GAM dispersion relations in Zonca & Chen (2008), Zonca *et al.* (1996) and Girardo *et al.* (2014). In the fluid limit, we can show that the dispersion relation equation (3.10) reduces to

$$\omega^2 = \left(\frac{3}{4} + \frac{\chi}{2} + \frac{\chi^2}{2} + b\tau\left(\frac{\chi^2}{4} + \frac{\chi}{2} + \frac{1}{4}\right)\right)\frac{v_t^2}{bR_0^2}. \tag{3.14}$$

If we consider the isotropic limit of this fluid dispersion relation, we obtain $\omega_{GAM}^2 = (7/4 + \tau)(v_t^2/R_0^2)$, which is the same GAM dispersion relation obtained using magnetohydrodynamics with a double adiabatic closure (Smolyakov *et al.* 2008). The GAMs are special types of sound waves and, as sound waves, their frequency strongly depends on the equilibrium pressure. Considering the magnetohydrodynamic description of GAMs with a double adiabatic closure, χ in our work is equivalent to the ratio $p_{\perp,0}/p_{\parallel,0}$, with $p_{\perp,0}$ the equilibrium perpendicular pressure and $p_{\parallel,0}$ the equilibrium parallel pressure. So increasing χ for a fixed $p_{\parallel,0}$ is equivalent to changing the equilibrium perpendicular pressure, which directly modifies the GAM frequency due to its dependence on the equilibrium pressure. This explains the global growing dependence of both the growth rate and frequency on χ, which is evident in the figures presented below. The GAM frequency can be written in terms of the equilibrium parallel and perpendicular pressures as follows (neglecting τ):

$$\omega_{GAM}^2 = \left(\frac{3}{2} + \frac{p_{\perp,0}}{p_{\parallel,0}} + \frac{p_{\perp,0}^2}{p_{\parallel,0}^2}\right)\frac{p_{\parallel,0}}{\rho_0 R_0^2}, \tag{3.15}$$

where ρ_0 is the equilibrium mass density. The dispersion relation equation (3.10) can be written in the following form by substituting (3.11), (3.12) and (3.13) in (3.10):

$$\frac{1}{b\tau}\left[\frac{1}{q^2} + \frac{1}{2} + \chi + y^2 + \left(y^3 + y\chi + \frac{\chi^2}{2y}\right)Z(y)\right] + \left[\frac{1}{q^2} + \frac{1}{2} + \chi + \frac{yZ(y)}{q^2} + \left(\frac{y}{2} + y\chi + \frac{\chi^2}{2y}\right) + \frac{\chi^2}{4}Z(y)^2\right] = 0. \tag{3.16}$$

3.3. *Asymptotic behaviour: case $\tau \to 0$*

In this limit, the first term in the square brackets is large compared with the second term. Neglecting this second term, we recover the dispersion relation in Ren & Cao (2014):

$$\frac{1}{q^2} + \frac{1}{2} + \chi + y^2 + \left(y^3 + y\chi + \frac{\chi^2}{2y}\right)Z(y) = 0. \tag{3.17}$$

Figure 1 shows the frequency and growth rate obtained from the complete dispersion relation (3.10) (blue curve) and the same quantities obtained in the $\tau \to 0$ limit (red curve).

3.4. *Asymptotic behaviour: case $\tau \to \infty$*

In this limit, the terms in the second square brackets in (3.16) are larger in comparison with those in the first. So the dispersion relation reduces to

$$\frac{1}{q^2} + \frac{1}{2} + \chi + \frac{yZ(y)}{q^2} + \left(\frac{y}{2} + y\chi + \frac{\chi^2}{2y}\right) + \frac{\chi^2}{4}Z(y)^2 = 0. \tag{3.18}$$

https://doi.org/10.1017/S0022377823000016 Published online by Cambridge University Press

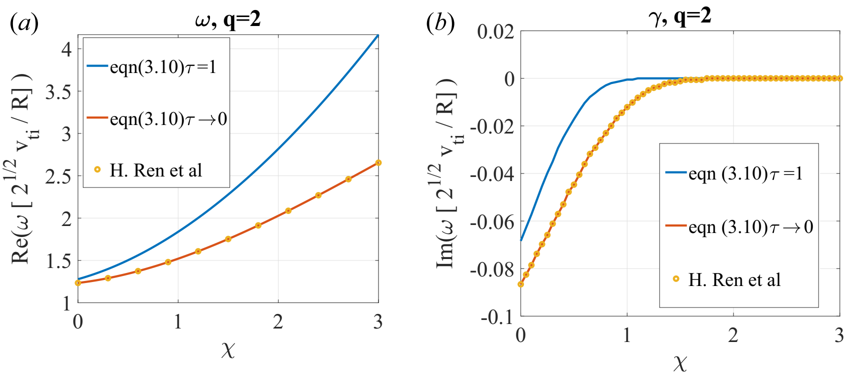

FIGURE 1. (*a*) Frequency. (*b*) Growth rate.

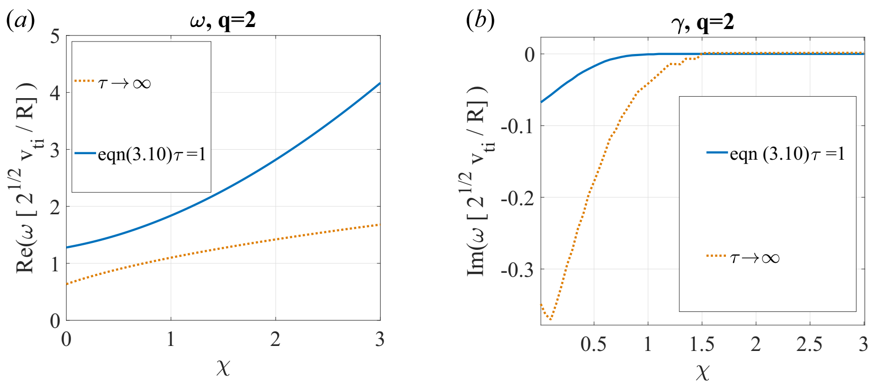

FIGURE 2. (*a*) Frequency. (*b*) Growth rate.

Figure 2 shows the frequency and growth rate obtained from the complete dispersion relation (3.10) (blue curve) and those obtained in the $\tau \rightarrow \infty$ limit (red dashed curve).

In the following sections, we solve the complete dispersion relation, (3.10), with values of τ that are more realistic for tokamak plasmas.

3.5. *Effect of ion temperature anisotropy on GAM frequency and growth rate*

The GAM frequency and growth rate increase with χ (figure 3). However, the growth rate saturates for values of the parameters for which the instability becomes marginally stable. This saturation occurs at lower values of χ for higher values of q. It should be noted that the growth rate at higher values of q is overestimated, since damping effects due to finite orbit width are not considered in our model. These effects tend to be more important when q increases (Biancalani *et al.* 2014). Similar results were obtained in Ren & Cao (2014). The regime of validity of our model is the plasma core. This is the region of excitation of energetic-particle-induced GAMs (EGAMs). Incidentally, the zonal flow residual level (Cho & Hahm 2021) can be enhanced by the anisotropic energetic particle distribution dominated by barely passing/barely trapped particles or by deeply trapped particles (Lu *et al.* 2019).

https://doi.org/10.1017/S0022377823000016 Published online by Cambridge University Press

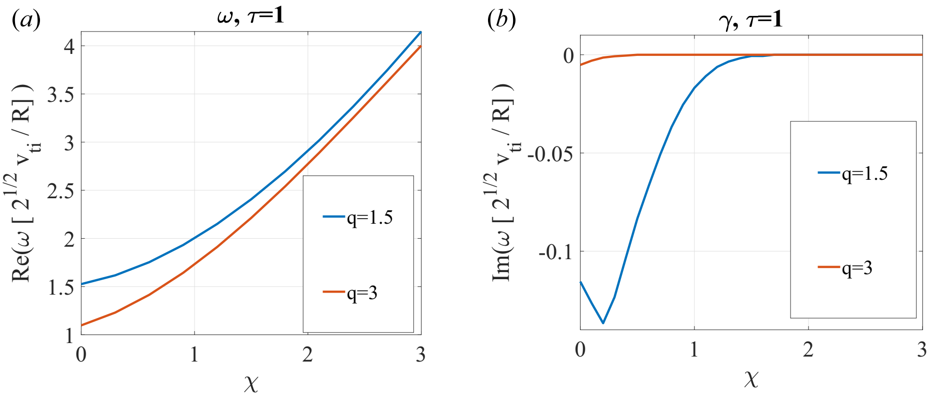

FIGURE 3. (*a*) Frequency. (*b*) Growth rate.

3.6. *Effects of electron to ion temperature ratio*

In this section, we study the effect of a finite τ (this parameter was neglected in Ren & Cao 2014). Figure 4(*a*,*b*) shows the effects of χ on GAM frequency and growth rate for two different values of τ. We observe, as expected, that these quantities are increasing functions of χ. However, there is a significant increase in frequency and growth rate with τ. Figure 4(*c*,*d*) shows the variation of GAM frequency and growth rate with τ for two values of χ. We recover the isotropic τ dependence of GAMs (i.e. increasing frequency with increasing τ). This effect is more pronounced for higher values of χ in the anisotropic case. Figure 5 shows the effect of τ on GAM frequency and growth rate for two different values of the safety factor q and for a fixed χ. We observe stronger damping for smaller values of q. This confirms the fact that even in the anisotropic case, GAMs are more stable in the core than at the edge of the tokamak plasma, where the safety factor q has large values. We can conclude from figures 4 and 5 that GAM frequency and growth rate significantly increase with τ and neglecting this parameter can lead to an underestimation of the frequency and to an overestimation of the damping rate.

4. Application to an experimentally relevant case

In this section, we apply the theory we have developed to a case of likely experimental relevance. For simplicity, we consider the case where the electron to ion temperature ratio is one ($\tau = 1$), which is compatible with experimental conditions. Sasaki *et al.* (1997) studied the ion temperature anisotropy in the reverse field pinch device EXTRAP-T2. In that work, $\chi \sim 0.5$ was measured. We here assume such values of χ are comparable with those that can be measured in tokamaks. To plot the GAM frequency spectrum for values of this parameter, we use the safety factor profile from the experimental benchmark test case selected for NonLinear Energetic-particle Dynamics EuroFusion project for Asdex Upgrade (NLED-AUG) (Vlad *et al.* 2021).

Figure 6 shows that the frequency spectrum of GAMs is very sensitive to the safety factor in the presence of ion anisotropy (Figure 7 shows the NLED-AUG safety factor profile used for these plots). This is particularly true closer to the plasma core where the GAM damping rate is almost an order of magnitude higher than in the isotropic case (damping due to finite orbit width which is important at higher values of q is not considered in this work). Even though GAMs are heavily damped in the core in the presence of anisotropy, as shown in figure 6, the core dynamic of GAMs is, however, important, since

https://doi.org/10.1017/S0022377823000016 Published online by Cambridge University Press

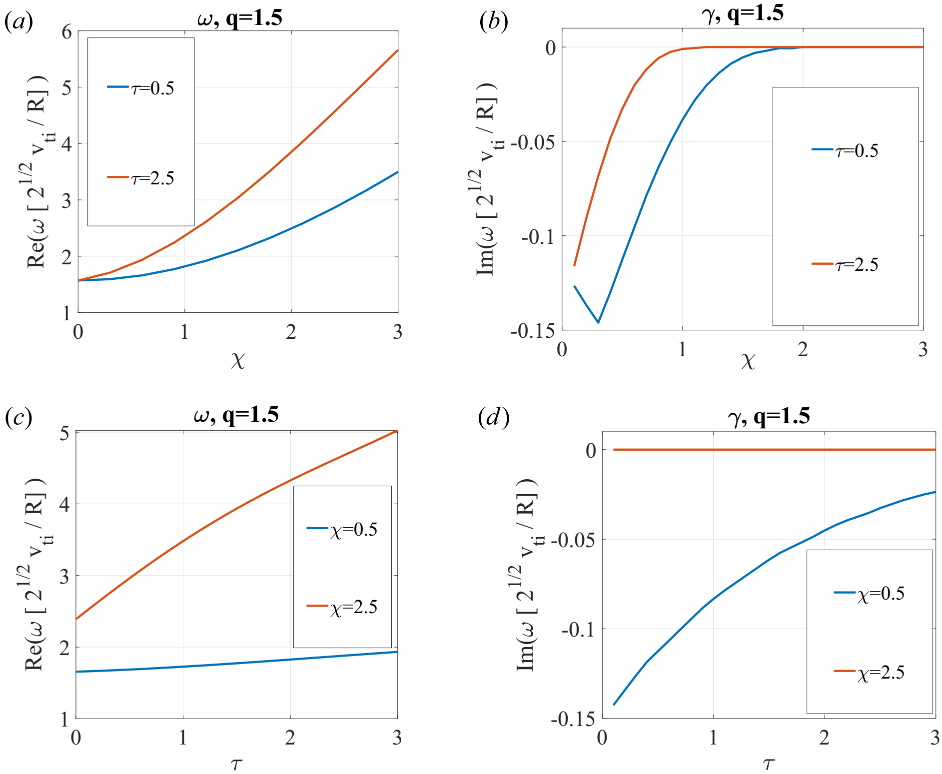

FIGURE 4. Effects of τ: (*a*,*c*) frequency; (*b*,*d*) growth rate.

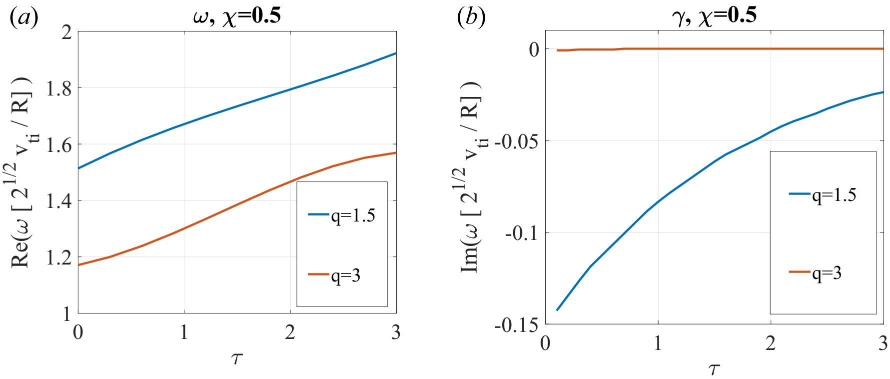

FIGURE 5. Effects of τ: (*a*) frequency; (*b*) growth rate.

it can significantly modify the interaction of GAMs and energetic particles in the core, which leads to the so-called EGAMs (Fu 2008; Vannini *et al.* 2021; Rettino *et al.* 2022).

5. Conclusion

Zonal structures are axisymmetric perturbations that are nonlinearly generated by turbulence in fusion plasmas. There are two main types of zonal flows, namely the zero-frequency zonal flow and its finite-frequency counterpart, the GAM. The GAMs are

https://doi.org/10.1017/S0022377823000016 Published online by Cambridge University Press

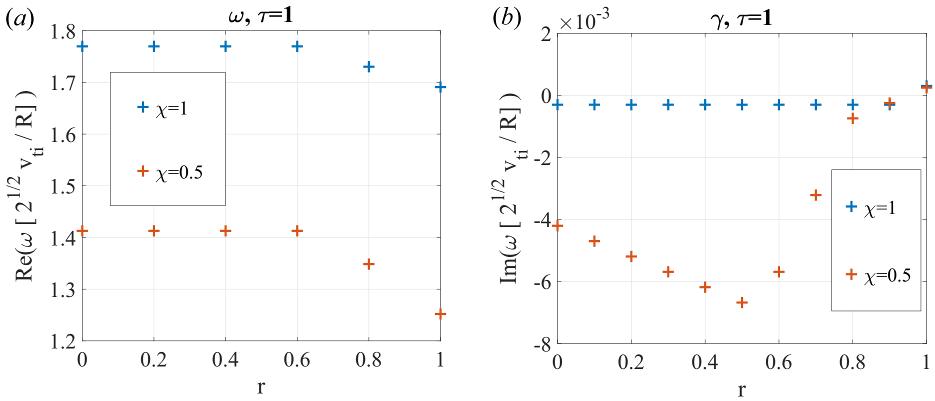

FIGURE 6. (*a*) Frequency versus radial position (r) and (*b*) growth rate versus radial position (r) for the set of parameters of potential experimental relevance discussed in § 4.

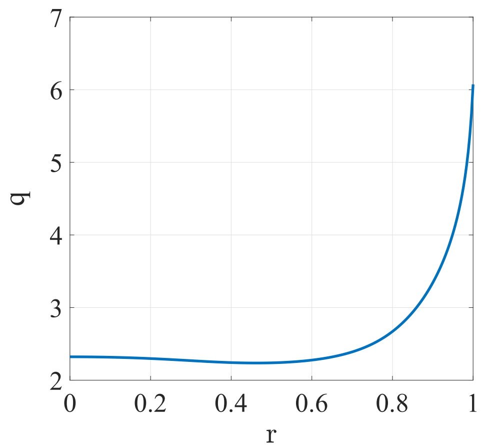

FIGURE 7. Safety factor profile.

unique to configurations with closed magnetic field lines with a geodesic curvature, like tokamaks. The GAM frequency is of the order of the ion sound frequency, and its major damping mechanism in fusion plasma is collisionless damping (ion Landau damping). The GAMs are of interest to future magnetic fusion devices due to their potential role in regulating microscopic turbulence and its associated heat and particle transport.

In this work we revisited the linear gyro-kinetic theory of GAMs with adiabatic electrons described by a Maxwellian distribution function by including the effects of kinetic ions displaying a gyro-tropic temperature anisotropy modelled with a bi-Maxwellian distribution. We thus extended the linear GAM theory with an anisotropic ion temperature to include a general value of the electron to ion temperature ratio and we derived a general linear dispersion relation for an arbitrary ion distribution function. In the appropriate limit of a negligible electron to ion temperature ratio, we thus recovered the GAM dispersion relation in Ren & Cao (2014). Solving the dispersion relation for the GAM frequency and damping rate for the more general case of interest here, we found that the ion temperature anisotropy yields non-negligible changes to both the GAM frequency and damping rate, as both tend to be increasing functions of $\chi = T_{\perp,i}/T_{\parallel,i}$. The ion Landau

https://doi.org/10.1017/S0022377823000016 Published online by Cambridge University Press

damping is confirmed to be stronger for smaller values of the safety factor. These features become more pronounced when a finite electron to ion temperature ratio is considered. The values of the frequency and growth rate for a given χ increase significantly as $\tau = T_e/T_i$ increases. Hence, the effect of τ on GAM dynamics is not negligible and must be included in a complete model.

We applied our theory to a scenario of potential experimental relevance by using the safety factor profile from the NLED-AUG experimental benchmark test case and assuming the ion temperature anisotropy in tokamaks is close to that measured in the reversed field pinch device EXTRAP-T2. Plotting the frequency spectrum and the damping rate as a function of position (while restricting for simplicity to the case of equal total electron and ion temperature), we find that in this scenario the core dynamics of GAMs is significantly modified in the presence of ion temperature anisotropy. Such a modification of the core dynamics of GAMs can impact the the interaction of GAMs and energetic particles in the plasma core.

In future works, we shall extend this linear theory of GAMs with inclusion of ion anisotropy effects in order to study the interaction of GAMs and energetic particles in the plasma core (EGAMs), since we have seen that the linear core dynamics of GAMs in relevant experimental scenarios is significantly modified by the ion temperature anisotropy.

Acknowledgements

The authors are grateful to E. Gravier and M. Lesur (IJL, Nancy, France), to G. Dif-Pradalier and X. Garbet (IRFM, CEA, France), to W. Bin and S. Schmuck (ISTP, CNR, Italy), to F. Zonca (CNPS, Frascati, Italy) and to X. Wang and Z. Lu (IPP, Garching, Germany) for useful discussions and remarks.

Editor P. Ricci thanks the referees for their advice in evaluating this article.

Funding

This work was partially supported by the Lorraine Université d'Excellence Doctorate funding (project R01PKJUX-PHD21) belonging to the initiative I-SITE LUE and by the R&D Program through Korea Institute of Fusion Energy (KFE) funded by the Ministry of Science, ICT and Future Planning of the Republic of Korea (no. KFE-EN2241-8). Part of this work was carried out within the framework of the EUROfusion Consortium, funded by the European Union via the Euratom Research and Training Programme (Grant Agreement no. 101052200 EUROfusion). Views and opinions expressed here are, however, those of the authors only and do not necessarily reflect those of the European Union or the European Commission. Neither the European Union nor the European Commission can be held responsible for them. Numerical calculations for this work were partially performed on the cluster Explor of the Maison de la simulation Lorraine (we are grateful for the partial time allocation under project no. 2019M4XXX0978) and on the MARCONI FUSION HPC system at CINECA.

Declaration of interests

The authors report no conflict of interest.

REFERENCES

BIANCALANI, A., BOTTINO, A., LAUBER, P. & ZARZOSO, D. 2014 Numerical validation of the electromagnetic gyrokinetic code NEMORB on global axisymmetric modes. *Nucl. Fusion* **54**, 104004.

CERRI, S.S., HENRI, P., CALIFANO, F., DEL SARTO, D., FAGANELLO, M. & PEGORARO, F. 2013 Extended fluid models: pressure tensor effects and equilibria. *Phys. Plasmas* **20**, 112112.

CHAKRABARTI, N., GUZDAR, P.N., KLEVA, R.G., SINGH, R., KAW, P.K., NAULIN, V. & RASMUSSEN, J.J. 2010 Geodesic acoustic mode in toroidal plasma. *AIP Conf. Proc.* **1308**, 108.

CHEN, L. & ZONCA, F. 2007 Nonlinear equilibria, stability and generation of zonal structures in toroidal plasmas. *Nucl. Fusion* **47**, 886–891.

CHO, Y.W. & HAHM, T.S. 2021 Effect of temperature anisotropy on residual zonal flow level. *Phys. Plasmas* **28**, 052303.

CONWAY, G.D., SMOLYAKOV, A.I. & IDO, T. 2022 Geodesic acoustic modes in magnetic confinement devices. *Nucl. Fusion* **62**, 013001.

DEL SARTO, D. & PEGORARO, F. 2018*a* Shear-induced pressure anisotropization and correlation with fluid vorticity in a low collisionality plasma. *Mon. Not. R. Astron. Soc.* **475**, 181.

DEL SARTO, D. & PEGORARO, F. 2018*b* Shear-induced pressure anisotropization and correlation with fluid vorticity in a low collisionality plasma. In *Un Comptes-Rendus de la 21e Rencontre du Non Linéaire, Paris 2018* (ed. E. Falcon, M. Lefranc, F. Ptrluis & C.-T. Pham) vol. 21, pp. 13–18. Université Paris Diderot, Non-Linéaire Publications.

DEL SARTO, D., PEGORARO, F. & CALIFANO, F. 2016 Pressure anisotropy and small spatial scales induced by velocity shear. *Phys. Rev.* E **93**, 053203.

FU, G.Y. 2008 Energetic-particle-induced geodesic acoustic mode. *Phys. Rev. Lett.* **101**, 185002.

GAO, Z. 2013 Collisional damping of the geodesic acoustic mode. *Phys. Plasmas* **20**, 032501.

GARBET, X., FALCHETTO, G., OTTAVIANI, M., SABOT, R., SIRINELLI, A. & SMOLYAKOV, A. 2006 Coherent modes in the acoustic frequency range in tokamaks. *AIP Conf. Proc.* **871**, 342.

GIRARDO, J., ZARZOSO, D., DUMONT, R., GARBET, X., SARAZIN, Y. & SHARAPOV, S. 2014 Relation between energetic and standard geodesic acoustic modes. *Phys. Plasmas* **21**, 092507.

GRANDGIRARD, V., GARBET, X., EHRLACHER, C., BIANCALANI, A., BOTTINO, A., NOVIKAU, I., ASAHI, Y., CASCHERA, E., DIF-PRADALIER, G., DONNEL, P., *et al.* 2019 Linear collisionless dynamics of the gam with kinetic electrons: comparison simulations/theory. *Phys. Plasmas* **26**, 122304.

HASEGAWA, A., MACLENNAN, C.G. & KODAMA, Y. 1979 Nonlinear behavior and turbulence spectra of drift waves and Rossby waves. *Phys. Fluids* **22**, 2122.

HASSAM, A.B. & KLEVA, R.G. 2011 Double adiabatic theory of collisionless geodesic acoustic modes in tokamaks. arXiv:1109.0057.

HOLE, M.J., VON NESSI, G., FITZGERALD, M, MCCLEMENTS, K.G., SVENSSON, J. & THE MAST TEAM 2001 Equilibrium analysis of tokamak discharges with anisotropic pressure. *Plasma Phys. Control. Fusion* **43**, 1441–1456.

HOLE, M.J., VON NESSI, G., FITZGERALD, M., MCCLEMENTS, K.G., SVENSSON, J. & THE MAST TEAM 2011 Identifying the impact of rotation, anisotropy, and energetic particle physics in tokamaks. *Plasma Phys. Control. Fusion* **53**, 074021.

KAUFMAN, A.N. 1960 Plasma viscosity in a magnetic field. *Phys. Plasmas* **3**, 610.

LU, Z.X., WANG, X., LAUBER, P., FABLE, E., BOTTINO, A., HORNSBY, W., HAYWARD-SCHNEIDER, T., ZONCA, F. & ANGIONI, C. 2019 Theoretical studies and simulations of mode structure symmetry breaking in tokamak plasmas in the presence of energetic particles. *Plasma Phys. Control. Fusion* **61**, 044005.

MACMAHON, A. 1965 Finite gyro radius corrections to the hydromagnetic equations for a vlasov plasma. *Phys. Plasmas* **3**, 610.

MING, Y., ZHOU, D. & WAMG, W. 2018 Geodesic acoustic modes in tokamak plasmas with anisotropic distribution and a radial equilibrium electric field. *Plasma Sci. Technol.* **20**, 085101.

NOVIKAU, I., BIANCALANI, A., BOTTINO, A., CONWAY, G.D., GURCAN, O.D., MANZ, P., MOREL, P., POLI, E., DI SIENA, A. & ASDEX UPGRADE TEAM 2017 Linear gyrokinetic investigation of the geodesic acoustic modes in realistic tokamak configurations. *Phys. Plasmas* **24**, 122117.

QIU, Z., CHEN, L. & ZONCA, F. 2009 Collisionless damping of short wavelength geodesic acoustic modes. *Plasma Phys. Control. Fusion* **51**, 012001.

REN, H. 2015 Geodesic acoustic mode in anisotropic plasma with heat flux. *Phys. Plasmas* **22**, 102505.

REN, H. & CAO, J. 2014 Geodesic acoustic mode in anisotropic plasmas using adiabatic model and gyro-kinetics equation. *Phys. Plasmas* **21**, 122512.

RETTINO, B., HAYWARD-SCHNEIDER, T., BIANCALANI, A., BOTTINO, A., LAUBER, P., CHAVDAROVSKI, I., VANNINI, F. & JENKO, F. 2022 Gyrokinetic modelling of anisotropic energetic particle driven instabilities in tokamak plasmas. *Nucl. Fusion* **62**, 076027.

SASAKI, K., HORLING, P., FALL, T., BRZOZOWSKI, J.H., BRUNSELL, P., HOKIN, S., TENNFORS, E., SALLANDER, J., DRAKE, J.R., INOUE, N., *et al.* 1997 Anisotropy of ion temperature in a reversed-field-pinch plasma. *Plasma Phys. Control. Fusion* **39**, 333–338.

SMOLYAKOV, A.I., GARBET, X., FALCHETTO, G. & OTTAVIANI, M. 2008 Multiple polarization of geodesic curvature induced modes. *Phys. Lett.* A **372**, 6750–6756.

SUGAMA, H. & WATANABE, T.H. 2006 Collisionless damping of geodesic acoustic modes. *J. Plasma Phys*. **72**, 825.

THOMPSON, W.B. 1961 The dynamics of high temperature plasmas. *Phys. Plasmas* **3**, 610.

VANNINI, F., BIANCALANI, A., BOTTINO, A., HAYWARD-SCHNEIDER, T., LAUBER, P., MISHCHENKO, A., POLI, E., VLAD, G. & ASDEX UPGRADE TEAM 2021 Gyrokinetic investigation of the nonlinear interaction of Alfvén instabilities and energetic particle-driven geodesic acoustic modes. *Phys. Plasmas* **28**, 072504.

VLAD, G., WANG, X., VANNINI, F., BRIGUGLIO, S., CARLEVARO, N., FALESSI, M.V., FOGACCIA, G., FUSCO, V., ZONCA, F., BIANCALANI, A., *et al.* 2021 A linear benchmark between HYMAGYC, MEGA and ORB5 codes using the NLED-AUG test case to study Alfvénic modes driven by energetic particles. *Nucl. Fusion* **61**, 116026.

WINSOR, N., JOHNSON, J.L. & DAWSON, J.M. 1968 Geodesic acoustic waves in hydromagnetic systems. *Phys. Fluids* **11**, 2448.

ZARZOSO, D., GARBET, X., SARAZIN, Y., DUMONT, R. & GRANDGIRARD, V. 2012 Fully kinetic description of the linear excitation and nonlinear saturation of fast-ion-driven geodesic acoustic mode instability. *Phys. Plasmas* **19**, 022102.

ZHANG, M. & ZHOU, D. 2010 Magnetic components of geodesic acoustic modes in plasmas with anisotropic ion distribution. *Plasma Sci. Technol*. **12**, 6–10.

ZONCA, F. & CHEN, L. 2008 Radial structures and nonlinear excitation of geodesic acoustic modes. *Europhys. Lett*. **83**, 35001.

ZONCA, F., CHEN, L. & SANTORO, R.A. 1996 Kinetic theory of low-frequency Alfvén modes in tokamaks. *Plasma Phys. Control. Fusion* **38**, 2011.